

Rapid, one-step fabrication and loading of nanoscale 1,2-distearoyl-sn-glycero-3-phosphocholine liposomes in a simple, double flow-focusing microfluidic device

Ryan V. Tien Sing Young¹ and Maryam Tabrizian^{1,2,a)}

¹Department of Biomedical Engineering, McGill University, Duff Medical Building, Montreal, Quebec H3A 2B4, Canada

²Faculty of Dentistry, McGill University, Strathcona Anatomy & Dentistry Building, Montreal, Quebec H3A 2B2, Canada

(Received 6 May 2015; accepted 25 June 2015; published online 1 July 2015)

Liposomes are currently well-established as biocompatible delivery vehicles for numerous compounds. However, conventional manufacturing tends to rely on time-consuming processes, costly equipment, unstable reaction parameters, and numerous pre- and post-processing steps. Herein, we demonstrate a microscope-slide-sized alternative: a double flow-focusing microfluidic geometry capable of sub-hour synthesis and controlled loading of tunable liposomes. Using phospholipid 1,2-distearoyl-sn-glycero-3-phosphocholine as the bilayer constituent, the effect of varying the dissolved lipid concentration and flow rate ratio on synthesized liposome diameters was investigated and the encapsulation of fluorescent hydrophobic drug model ergost-5,7,9(11),22-tetraen-3 β -ol was performed to ascertain the potential of this device as a loading platform. © 2015 AIP Publishing LLC. [<http://dx.doi.org/10.1063/1.4926398>]

I. INTRODUCTION

A. Background

Liposomes, since their discovery by Bangham *et al.* in 1965,¹ have been utilized for a wide range of applications ranging from drug delivery vehicles^{2,3} to cosmeceuticals⁴ to food nanotechnology.⁵ Defined as single or multiple bilayered, spheroidal vesicles typically composed of phospholipid molecules, they form when these phospholipids self-assemble hydrophobic tail to hydrophobic tail into a bilayer sheet and eventually bend upon themselves.^{6,7} The liposome configuration, which consists of a/multiple hydrophilic core/s and a/multiple hydrophobic bilayer/s, allows for the encapsulation of a variety of bioactive agents, including amphiphilic compounds.⁸ As a delivery vehicle, the use of liposomes offers many advantages including longer circulation times within the body, protection and controlled release of the encapsulated molecules, and the ability to overcome biological barriers to achieve targeted delivery.⁹ Moreover, the particle diameters have been shown to play an important role on their circulation time within the body and eventual elimination.¹⁰

Conventional methods for liposome preparation usually revolve around three processes: dissolving the lipid in a solvent, dispersing the mixture in an aqueous phase, and post-processing the synthesized vesicles to achieve desired sizes and conformations.¹¹ The main bulk methods include thin-film hydration, solvent injection, reverse-phase evaporation, and detergent depletion, all occasionally followed by polycarbonate filter extrusion.¹² Encapsulation occurs either passively or actively; the former occurring before liposomes have formed and the latter after vesicle formation.¹³ The main drawbacks with synthesis via these bulk methods are the processing times, the difficulty in obtaining relatively monodisperse products without post-processing,

^{a)} Author to whom correspondence should be addressed. Electronic mail: Maryam.Tabrizian@mcgill.ca

the large reagent volumes required, and the multiple platforms necessary for passive or active encapsulation.

The application of microfluidic principles could address some of these issues. Indeed, since Whitesides *et al.*¹⁴ pioneered the use of low-cost microfluidics using poly(dimethylsiloxane) (PDMS) at the end of the last century, it has been used as a versatile tool for applications such as drug discovery using organ-on-a-chip platforms¹⁵ and as affordable solutions for point-of-care diagnostics.¹⁶ In the realm of liposomes, microfluidics has been used in an attempt to resolve some of the aforementioned bulk technique drawbacks. Such adaptations include electroformation, flow focusing, double emulsion templates, and transient membrane ejection. For an in depth summary, the authors refer the reader to the excellent review by van Swaay and deMello.¹⁷

Hydrodynamic flow focusing (HFF) is a process whereby the central stream of dissolved phospholipid is focused by an aqueous buffer, resulting in the outwards diffusion of the solvent into the aforementioned buffer, ultimately dropping the solvent concentration and consequently forming liposomes.¹⁸ Building upon the HFF work done previously by Jahn *et al.*,^{18,19} a recent development of notable interest is the work done by Hood *et al.* regarding the development of a single-step liposomal preparation technique using “microfluidic remote loading.”²⁰ In addition to the HFF process, their device also incorporated an active loading step: a counterflow microdialysis component for the generation of a transmembrane ion gradient. Albeit an innovative platform, the latter resulted in a fairly complex multi-tiered system. Defining encapsulation efficiency as the amount of drug retained within the liposome compared to the initial added amount, this group achieved encapsulation efficiencies greater than 50% for sub-250 nm vesicles loaded with acridine orange hydrochloride, an amphiphatic drug model, and doxorubicin, a compound used for cancer therapy.

In this “Fabrication and Laboratory Methods” article, we demonstrate a straightforward, continuous-flow, microfluidic geometry, for the one-step, rapid synthesis and loading of nano-/micro-scale liposomes of predictable size. This device only consists of a simple, double HFF configuration. For this initial prototype, 1,2-distearoyl-sn-glycero-3-phosphocholine (DSPC) was chosen as the bilayer constituent. The particle diameters were evaluated with respect to phospholipid concentration and flow rates. Subsequently, ergost-5,7,9(11),22-tetraen-3 β -ol (DHE), a fluorescent hydrophobic drug model, was then encapsulated within the DSPC liposomes.

B. Design validation

The emphases of this design (see Fig. 1) were above all else simplicity and low-cost. The device footprint was constrained to that of readily available glass microscope slides (i.e., 25 mm \times 75 mm). A microfluidic, HFF, planar channel geometry, as initially described by Jahn *et al.*,¹⁸ was the motivation for this device. The synthesized particles rely primarily on diffusion between the fluid streams; by solvent diffusion out of the focused streamlet, the formation and subsequent bending of the bilayer sheets are promoted. Liu *et al.*²¹ determined that the optimal junction angle to achieve the smallest particles for flow focusing was of 30° from the main channel, a feature which was incorporated as an essential channel geometry component. Additionally, as opposed to the traditional setup of supplying the focusing sheath via two separate inlets, these were joined into a single inlet for space saving and for more evenly distributed flow. Furthermore, rather than sharp corners, a smooth outermost curvature was implemented in order to diminish flow perturbations within the channels. To allow for on-chip loading, the HFF pattern was then duplicated. The channels from the leftmost inlet (Fig. 1(b)) have a second outwards curvature to provide the optimal focusing angle of 30°. The inclusion of the aforementioned elements into our design allowed not only for a simplified design but also aesthetically, for a more streamlined, minimalist device.

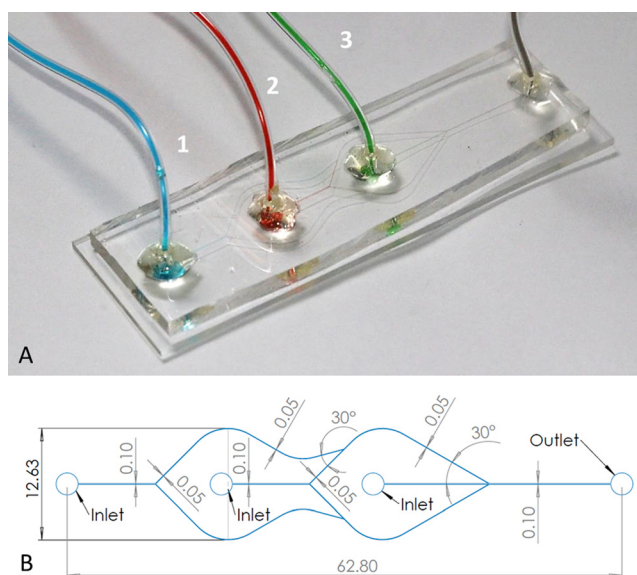


FIG. 1. (a) Double hydrodynamic flow focusing device. Inlets labeled 1, 2, and 3. (b) Technical diagram of pattern (all dimensions in mm).

II. EXPERIMENTAL

A. Materials

Negative photoresist, SU-8 2050, was purchased from Microchem Corp. (Boston, MA, USA). Sylgard 184 elastomer kits, consisting of a prepolymer and a curing agent of PDMS, were purchased from Dow Corning Corp. (Saint-Laurent, QC, Canada). Tygon 0.020" ID microbore tubing was purchased from Cole-Parmer Canada, Inc. (Montreal, QC, Canada). Quick setting epoxy adhesive was purchased from LePage-Henkel (Mississauga, ON, Canada). Analytical grade 2-propanol, acetone, and methanol (MeOH) as well as glass microscope slides were purchased from Fisher Scientific (Waltham, MA, USA). Anhydrous ethyl alcohol (EtOH) was purchased from GreenField Specialty Alcohols, Inc. (Brampton, ON, Canada). DHE and trichloro(1H,1H,2H,2H-perfluorooctyl)silane were purchased from Sigma Aldrich (Oakville, ON, Canada). DSPC was purchased from Avanti Polar Lipids, Inc. (Alabaster, AL, USA). Ultra-pure water (MilliQ) from a Millipore filtration system (resistivity of $>18.2 \text{ M}\Omega \text{ cm}$) was used for all experiments.

B. Design and fabrication of microfluidic chip

The pattern for the microfluidic design was created using SolidWorks 2013 (Dassault S.A.—Vélizy, France). A detailed break-down of device fabrication is presented in Fig. 1S in supplementary material, Ref. 31. Negative photoresist was spin-coated onto a silicon wafer to achieve a thickness of $100 \mu\text{m}$. Conventional ultraviolet photolithography was performed using a channel-patterned chrome photomask to fabricate the mould. It was then silanized by chemical vapour deposition using trichloro(1H,1H,2H,2H-perfluorooctyl)silane to aid with the demoulding. Via standard soft lithography, the PDMS mixture, prepared following the manufacturer's protocol, was poured onto the patterned wafer. The polymer was cured, peeled off, cut to size, and hole-punched to form inlet and outlet conduits. Cleaned slides and the moulded PDMS sections were then treated with oxygen plasma and pressed together to form an irreversible bond. Tygon tubing was inserted into the inlet and outlet ports, and the junctions were then sealed using epoxy (see Fig. 1(a)). Three 21 gauge dispensing needles (Howard Electronic Instruments, Inc.—El Dorado, KS, USA) were attached to the inlet tubes as quick-connects for the syringes (BD Medical—Mississauga, ON, Canada). The flow was controlled using

multi-channel syringe pumps (Nexus 3000, Chemyx, Inc.—Stafford, TX, USA and/or KDS220, KD Scientific, Inc.—Holliston, MA, USA).

C. Liposome synthesis

The phospholipid-solvent mixtures (DSPC:EtOH) were prepared using DSPC dissolved directly into EtOH at various concentrations. They were prepared in glass vials (VWR International—Radnor, PA, USA) and stored at 4 °C until use. For the encapsulation studies, a 2 mg/ml stock solution of fluorescent DHE was prepared as per the manufacturer's protocol by adding 2.5 ml of MeOH to a 5 mg vial of DHE and stored at −20 °C. Detailed batch descriptions can be found in Table S1 (see supplementary material in Ref. 31).

1. Microfluidic liposome synthesis (unloaded and loaded)

For the unloaded experiments, inlet 1 was blocked, MilliQ water flowed through inlet 2, and DSPC:EtOH flowed through inlet 3. For the runs correlating diameter with lipid concentration, DSPC:EtOH solutions at concentrations of 1, 3, 6, 10, and 15 mg/ml were prepared. The flow rate ratios (FRRs), defined as the total volumetric flow rate divided by the focused sheath flow rate, investigated were 20 and 150. For the experiment correlating diameter with FRR, concentration was fixed to 3 mg/ml and FRRs of 5, 10, 20, 30, 40, 50, 100, and 150 were chosen.

For the encapsulation investigation, the FRR was set to 50 and the DSPC:EtOH concentration was 3 mg/ml. The control, batch A, was prepared by flowing MilliQ water, 3 mg/ml DSPC:EtOH, and MeOH through inlets 1, 2, and 3, respectively. Batch B consisted of the same setup, except for 0.5 mg/ml DHE:MeOH flowing through inlet 3, i.e., loaded. Active loading of the microfluidic-synthesized liposomes (batch E) was performed by obtaining nanoliposomes in the same setup as per batch A, subsequently injecting 0.5 mg/ml DHE:MeOH at a ratio of 1:40 (DHE:MeOH to liposome sample volume) and allowing for diffusion over 24 h.

2. Conventional liposome synthesis and active loading

The liposomes were conventionally synthesized via a comparable simple ethanol injection method. A syringe pump was used to inject 1 ml of 3 mg/ml DSPC:EtOH at 10 μ l/min into a vial containing 20 ml of MilliQ water, achieving the same ratios as with the microfluidic synthesis (Table S1, batch C, Ref. 31). Active loading was performed as described in Sec. IIC 1 with the same subsequent DHE:MeOH injection process into the products of ethanol injection (Table S1, batch D, Ref. 31).

D. Particle size measurement, imaging, and spectrophotometric analysis

The liposome diameters were measured by dynamic light scattering (DLS) using a ZetaPALS Zeta Potential Analyzer (Brookhaven Instruments Corp.—Holtsville, NY, USA). An inverted microscope (Eclipse TE 2000-U, Nikon Corp.—Mississauga, ON, Canada), with fluorescence capabilities, was used to visualize the liposomes as well as the fluorescence emission from the DHE. All images were captured using a CCD camera (Retiga-2000R, Qimaging—Surrey, BC, Canada) and Nikon NIS-Elements D software. A Molecular Devices SpectraMax i3 Multi-Mode Microplate Reader (Sunnyvale, CA, USA) was used to measure the fluorescence intensity of the samples.

E. Statistical analysis

All data are expressed as mean \pm standard deviation of at least 3 independent replicates per group. Statistical analyses were performed for multiple comparisons via one-way analysis of variance and Student's *t*-test was used for direct comparison between results. Differences were considered significant for $p < 0.05$.

III. RESULTS AND DISCUSSION

HFF has previously been used to produce a myriad of nanoparticles for potential drug delivery systems, ranging from polymers²² to nanoemulsions.²³ The use of HFF as a synthesis method is advantageous not only in its inherent simplicity as compared to other methods but also in its ability to produce particles of various diameters by simply adjusting the flow rate. In this work, we introduce a double HFF microfluidic geometry for DSPC liposome synthesis and loading. Moreover, we determine the correlations between particle diameter with respect to DSPC:EtOH concentration and with respect to FRR.

Fig. 2 illustrates the effect of varying lipid concentration (Fig. 2(a)) and FRR (Fig. 2(b)), both with respect to particle diameter, as well as illustrations (Figs. 2(c) and 2(d)) demonstrating flows using food dye. For a FRR of 20 (see Fig. 2S³¹), the particle diameters obtained via DLS indicated concentrations of 1 and 3 mg/ml resulted in the smallest particle diameters, with no significant difference between them. For concentrations of 6 and 10 mg/ml, there was almost a doubling in the size of the liposomes. For the 15 mg/ml batch, they were approximately 40% larger than the 3 mg/ml liposomes. Subsequently, the same concentrations of DSPC:EtOH were evaluated at a FRR of 150. A similar pattern was observed, this time with the 3 mg/ml producing significantly smaller lipid nanoparticles (360.2 ± 32.0 nm), and the higher concentrations resulting in vesicles nearly twice the size of the former (Fig. 2(a)).

To date, the formation mechanism of liposomes in injection methods is not fully understood. Other investigations using phosphatidylcholine-based lipids as the bilayer component demonstrated an increase in liposome size with increasing dissolved lipid concentration,^{24–26} or a bell-shaped trend, as demonstrated by Balbino *et al.*²⁷ Herein, the use of DSPC demonstrated a jigsaw pattern with increasing concentration. The latter, in combination with the effects of liposome formation below the transition temperature, as demonstrated by Zook and Vreeland,²⁶ could explain this trend. Further investigation into the formation kinetics is required on this front.

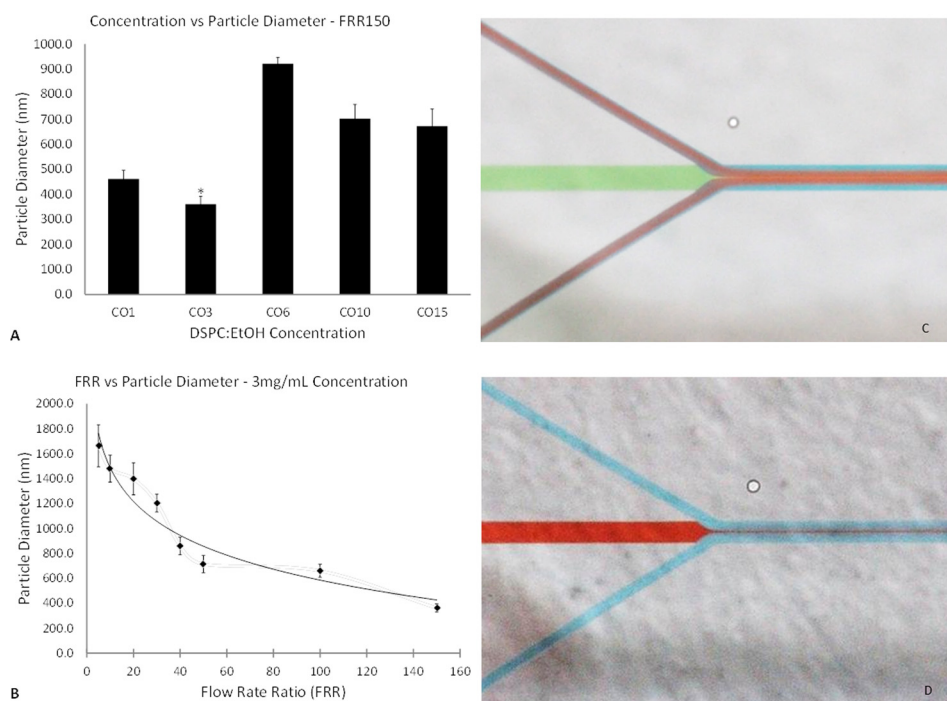


FIG. 2. DLS measurements for varying concentrations and FRR of DSPC:EtOH. Designation: CO##, where ## refers to dissolved lipid concentration. (a) Concentration vs particle diameter for FRR 150. (b) Correlation between flow rate ratio and particle diameter (fit: logarithmic). (c) Flow focusing at the primary junction using food dye. (d) Diffusion out of primary stream.

With a fixed phospholipid concentration and increasing FRRs, the DLS measurements indicated a trend of decreasing particle diameter with increasing FRR. All non-neighbouring results were statistically different, except for FRR 5 and FRR 20. With further extrapolation, one would expect to eventually see a minimum plateau being reached as FRRs continue to increase, as previously demonstrated with other liposome formulations.^{25,26,28} The formation of a very thin sample stream at higher FRRs (see Fig. 2(c)) and increased outwards diffusion (see Fig. 2(d)), also previously demonstrated by Jahn *et al.*,¹⁹ can account for the formation of smaller vesicles. However, the vesicles produced by our device were much larger than those reported in the latter. This is possibly due to the use of wider channels, as well as dissimilar phospholipid preparation procedures. With the present device iteration, at higher FRRs, the resulting solution was fairly dilute and as a result rather difficult to analyze both qualitatively and quantitatively.

After setting the concentration and FRR for liposome synthesis to 3 mg/ml and 50, respectively, DHE encapsulation was attempted. Approximately 3 ml of product was obtained in less than 1 h, with larger volumetric outputs, and in turn faster production times, achievable simply by increasing the fluid flow rates. In contrast to the methods devised by Jahn *et al.* and Hood *et al.*, the overall process is much shorter due to the omission of the 24 h chloroform dissolution step. Fluorescence images obtained from batches B and E are seen in Fig. 3, with fluorescent DHE used as a hydrophobic drug model. This compound has previously been used as a cholesterol analog for sterol trafficking studies²⁹ and has been proven to mimic cholesterol in bilayer structure and dynamics.³⁰ Batch E liposomes should not be affected by the loading time due to the minute volume of solvent present in the mixture. The fluorescence images in Figs. 3(a) and 3(b) imply that the DHE was successfully encapsulated within the liposomes. Optical microscopy (not shown here) comparing batches B and E to stock DHE solution confirmed the absence of any free DHE molecules. Particles synthesized via the microfluidic flow-focusing method, batches A, B, and E, resulted in liposomes which were approximately 30% smaller in diameter compared to those made by means of the comparable conventional ethanol injection method, batches C and D (Figs. 3(c) and 3(e)). The HFF causes the formation of a thin central sheath, which due to the larger surface area to volume ratio, allows for greater solvent diffusion and ultimately smaller particles than those produced in a bulk setup. All nanoliposomes manufactured in groups A–E were smaller than those in our characterization experiments. This could have been caused either by the modified operational setup itself (i.e., utilizing inlets 1, 2, and 3, as opposed to just 2 and 3) or by-product of this modified setup, the longer area in which the diffusion could occur. It was also observed that the loading method, passive or active, did not affect the final size of the liposomes, as demonstrated by the DLS measurements of batches B and E in comparison to batch A.

The different batches were analyzed in a binary fashion via fluorescent spectrophotometry (Figs. 3(d) and 3(f)). Taking the relative fluorescence units (RFU) values for batch A as a

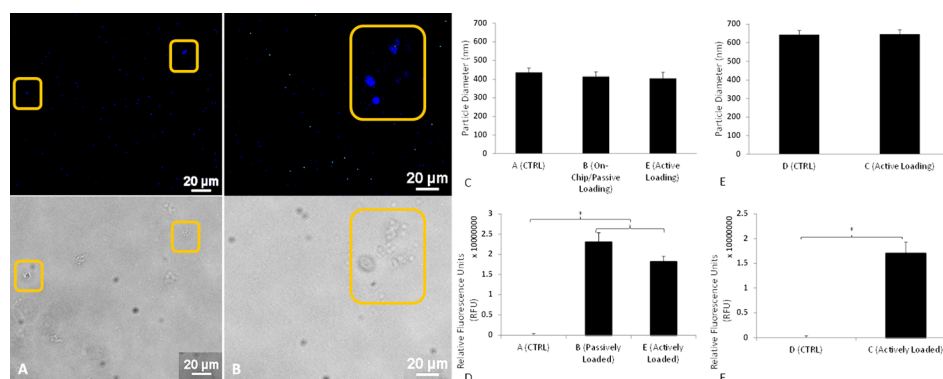


FIG. 3. Encapsulation study. Fluorescence and optical imaging for produced liposomes (20× Magnification): (a) Batch B, (b) Batch E. (c) and (d) Microfluidic liposomes, particle diameters, and fluorescence. (e) and (f) Conventional liposomes, particle diameters, and fluorescence.

baseline for microfluidic liposomes containing no DHE, the samples loaded with the fluorescent molecules, batches B and E, demonstrated significantly increased emission spectra values over the baseline readings. Conventionally, synthesized nanoliposomes, batches C and D, actively loaded and baseline, respectively, were also significantly different from one another in terms of adjusted RFU values.

These results indicate that this double flow-focusing geometry could be feasible for use as a low-cost, quick synthesis, and loading platform. The simplicity in geometry, ease of manufacturing, and minimal material requirements make this device an interesting alternative to many of the bulk production techniques. In addition to being used as a one-stop fabrication device, this microfluidic chip could be used as a test-bed for rapid prototyping optimal liposomal blends. The multi-faceted adjustability offers much greater control over many of the typical reaction parameters, from flow rate to reagent control.

Future iterations of this design should include addressing the highly dilute solutions obtained when creating the liposomes at high FRRs and testing encapsulation with hydrophilic and amphiphilic compounds, after which further quantification of the processing time should be obtained. More concentrated solutions could be achieved by creating channels with smaller widths, thus requiring smaller FRRs to achieve similar sheath compression, or even the inclusion of an expansion channel with multiple outlets to enable drainage of excess fluid. The reduction in channel widths could potentially also result in the formation of smaller nanoparticles, allowing for a wider range of applications. Furthermore, future work should include quantifying the encapsulation efficiency of DHE, as well as the encapsulation of therapeutic compounds. In addition to synthesizing and loading liposomes, it is hoped that the geometry of this simplistic device could potentially be utilized as a beneficial manufacturing platform for other types of nanoparticles such as polymeric compounds or emulsions.

IV. CONCLUSION

In this study, we have developed and demonstrated a straightforward microfluidic geometry incorporating an optimal flow-focusing angle as a proof-of-concept capable of continuous-flow synthesis and loading of DSPC liposomes. A simple, low-cost, and easily scalable in parallel, double flow-focusing device was utilized as a preliminary prototype. Herein, scalability refers to running multiple devices simultaneously. With our platform, we reduced the number of different apparatus required and reduced the amount of steps needed for the synthesis of liposomes. The initial study revealed an interesting trend regarding increasing the dissolved phospholipid concentration whereby the particle diameter decreases initially, suddenly rises, to ultimately decrease again. Additionally, we established a correlation between increasing the FRR and the resulting decrease in particle diameter. With further extrapolation, it is posited that the liposome size ultimately achieves a minimal plateau. The platform enabled the synthesis of particles with a range of diameters simply by adjusting the buffer flow rate. However, an excessive increase in FRR can lead to bursting of the Tygon inlets due to high pressures and the production of very dilute liposome solutions. Furthermore, we demonstrated the advantage of using a microfluidic method over a comparable conventional macro-scale technique to manufacture sub-500 nm particles loaded with a hydrophobic drug model. Moreover, the platform presents the possibility of multiple encapsulated agents in the synthesis of not only liposomes but also various nano-/microparticulate systems.

ACKNOWLEDGMENTS

The authors would like to acknowledge the NSERC-CREATE grant in Continuous Flow. The authors would also like to thank Dr. Jamal Daoud, Dr. Kristen Bowey, Dr. Amir Foudeh, and the Biomat'X Research Laboratories members for their time, patience, and invaluable advice, and Mr. Seddik Benhammadi for his assistance in the McGill Nanofab-Microtools facility.

¹A. D. Bangham, M. M. Standish, and J. C. Watkins, *J. Mol. Biol.* **13**(1), 238–252 (1965).

²T. M. Allen and P. R. Cullis, *Adv. Drug Delivery Rev.* **65**(1), 36–48 (2013).

- ³W. T. Al-Jamal and K. Kostarelos, *Acc. Chem. Res.* **44**(10), 1094–1104 (2011).
- ⁴Y. Rahimpour and H. Hamishehkar, *Expert Opin. Drug Delivery* **9**(4), 443–455 (2012).
- ⁵M. Reza Mozafari, C. Johnson, S. Hatziantoniou, and C. Demetzos, *J. Liposome Res.* **18**(4), 309–327 (2008).
- ⁶A. Jesorka and O. Orwar, *Annu. Rev. Anal. Chem.* **1**, 801–832 (2008).
- ⁷D. D. Lasic, *Biochem. J.* **256**(1), 1–11 (1988).
- ⁸V. P. Torchilin, *Nat. Rev. Drug Discovery* **4**(2), 145–160 (2005).
- ⁹K. Bowey, J. F. Tanguay, and M. Tabrizian, *Expert Opin. Drug Delivery* **9**(2), 249–265 (2012).
- ¹⁰L. D. Mayer, L. C. Tai, D. S. Ko, D. Masin, R. S. Ginsberg, P. R. Cullis, and M. B. Bally, *Cancer Res.* **49**(21), 5922–5930 (1989), available at <http://cancerres.aacrjournals.org/content/49/21/5922.long>.
- ¹¹C. Jaafar-Maalej, A. Elaissari, and H. Fessi, *Expert Opin. Drug Delivery* **9**(9), 1111–1127 (2012).
- ¹²A. Laouini, C. Jaafar-Maalej, I. Limayem-Blouza, S. Sfar, C. Charcosset, and H. Fessi, *J. Colloid Sci. Biotechnol.* **1**(2), 147–168 (2012).
- ¹³A. Akbarzadeh, R. Rezaei-Sadabady, S. Davaran, S. W. Joo, N. Zarghami, Y. Hanifehpour, M. Samiei, M. Kouhi, and K. Nejati-Koshki, *Nanoscale Res. Lett.* **8**(1), 102 (2013).
- ¹⁴D. C. Duffy, J. C. McDonald, O. J. A. Schueller, and G. M. Whitesides, *Anal. Chem.* **70**(23), 4974–4984 (1998).
- ¹⁵A. Polini, L. Prodanov, N. S. Bhise, V. Manoharan, M. R. Dokmeci, and A. Khademhosseini, *Expert Opin. Drug Discovery* **9**(4), 335–352 (2014).
- ¹⁶A. M. Foudeh, T. Fatanat Didar, T. Veres, and M. Tabrizian, *Lab Chip* **12**(18), 3249–3266 (2012).
- ¹⁷D. van Swaay and A. deMello, *Lab chip* **13**(5), 752–767 (2013).
- ¹⁸A. Jahn, W. N. Vreeland, M. Gaitan, and L. E. Locascio, *J. Am. Chem. Soc.* **126**(9), 2674–2675 (2004).
- ¹⁹A. Jahn, W. N. Vreeland, D. L. DeVoe, L. E. Locascio, and M. Gaitan, *Langmuir* **23**(11), 6289–6293 (2007).
- ²⁰R. R. Hood, W. N. Vreeland, and D. L. DeVoe, *Lab Chip* **14**(17), 3359–3367 (2014).
- ²¹K. Liu, L.-B. Zhao, Q. Zeng, Z.-X. Guo, J. Liu, and X.-Z. Zhao, paper presented at the 1st International Conference on Bioinformatics and Biomedical Engineering (ICBBE), 2007.
- ²²F. S. Majedi, M. M. Hasani-Sadrabadi, S. H. Emami, M. A. Shokrgozar, J. J. VanDersarl, E. Dashtimoghdam, A. Bertsch, and P. Renaud, *Lab Chip* **13**(2), 204–207 (2013).
- ²³S. L. Anna, N. Bontoux, and H. A. Stone, *Appl. Phys. Lett.* **82**(3), 364 (2003).
- ²⁴M. J. Kennedy, H. D. Ladouceur, T. Moeller, D. Kirui, and C. A. Batt, *Biomicrofluidics* **6**(4), 44119 (2012).
- ²⁵M. Mijajlovic, D. Wright, V. Zivkovic, J. X. Bi, and M. J. Biggs, *Colloids Surf., B* **104**, 276–281 (2013).
- ²⁶J. M. Zook and W. N. Vreeland, *Soft Matter* **6**(6), 1352–1360 (2010).
- ²⁷T. A. Balbino, N. T. Aoki, A. A. M. Gasperini, C. L. P. Oliveira, A. R. Azzoni, L. P. Cavalcanti, and L. G. de la Torre, *Chem. Eng. J.* **226**, 423–433 (2013).
- ²⁸A. Jahn, S. M. Stavis, J. S. Hong, W. N. Vreeland, D. L. DeVoe, and M. Gaitan, *ACS Nano* **4**(4), 2077–2087 (2010).
- ²⁹D. Wustner, L. Solanko, E. Sokol, O. Garvik, Z. Li, R. Bittman, T. Korte, and A. Herrmann, *Chem. Phys. Lipids* **164**(3), 221–235 (2011).
- ³⁰J. R. Robalo, A. M. do Canto, A. J. Carvalho, J. P. Ramalho, and L. M. Loura, *J. Phys. Chem. B* **117**(19), 5806–5819 (2013).
- ³¹See supplementary material at <http://dx.doi.org/10.1063/1.4926398> for soft lithography process, concentration vs particle diameter for FRR20, and batch characteristics.